Fall 2022

Investigation of Carbon Dioxide Oxidation Reaction Pathways on Rh(111) Via Reflection Absorption Infrared Spectroscopy (rairs)

Elizabeth A. Jamka

LOYOLA UNIVERSITY CHICAGO

INVESTIGATION OF CARBON DIOXIDE OXIDATION REACTION PATHWAYS ON RH(111) VIA REFLECTION ABSORPTION INFRARED SPECTROSCOPY (RAIRS)

A DISSERTATION SUBMITTED TO

THE FACULTY OF THE GRADUATE SCHOOL

IN CANDIDACY FOR THE DEGREE OF

DOCTOR OF PHILOSOPHY

PROGRAM IN CHEMISTRY AND BIOCHEMISTRY

BY

ELIZABETH A. JAMKA

CHICAGO, IL

AUGUST 2022

ACKNOWLEDGMENTS

I would like to thank everyone who help to make this dissertation possible. Starting with my committee chair and advisor, Dr. Daniel Killelea. I thank him for everything he has done and taught me to get to this point. His willingness to take a chance on me when I switched groups and specialties late in the program, will always mean the world to me. I could not have done it without him and his support. To the professors in the Chemistry and Biochemistry Department at Loyola University Chicago, especially Dr. Daniel Graham, Dr. Daniel Becker, Dr. Patrick Daubenmire and Dr Joerg Zimmermann who all provided key advice and guidance as past and current members of my yearly progress committee and defense committee. To all the undergrads I have worked with, George, Faith, Christina, Allison, JA, and Evelyn; I cannot thank you enough for your help and friendship during the years. I could not have gotten everything done without you all and I am and always be super proud of all of you. I cannot wait to see what you pursue in the future. Dr Katerina Binaku, you have been a wonderful mentor and friend through the years, I hope to one day help students, in and out of the lab, as you have helped me.

I would also like to thank Loyola University Chicago for providing the funds with which to complete my research and writing. The Teaching Assistantships were the part of the job that I thoroughly enjoyed. I loved helping students through their laboratory classes and helping the instructors throughout the semesters. The Teaching Scholars Fellowship for the 2021-2022 school year allowed me to focus on the writing process and continue to develop my teaching

skills. I also met wonderful colleagues and learned so much from them.

Finally, I must thank my friends and family. Dr Carly Hanson, Dr Aero ‘Kathryn’ Renyer, and Dr Adri Lugosan; without your help and friendship through the years I do not know how I could have gotten to this point. The lunch, coffee breaks, movie and taco nights will always be needed, welcomed, and full of great memories. Emily Strentz and Katie Wellington, you two are my biggest cheering squad, my rock through the tough times, and my favorite travel buddies. Thank you for always believing in me and helping me get to this point. To my mother and father, Nancy and Jim, I would be nothing without you both. Words cannot describe how grateful I am to have you both as parents and to have both of you present for these last major school related milestones. Dad, this is just as much for you as it is me. And finally to my sister, Julia, my favorite sister and favorite carpool buddy. I will always strive to be my best version of myself because of you. Thank you all.

For those who believed I couldn’t.
But most importantly, for those who believed I could.

You do not yield.

—*Kingdom of Ash,* Sarah J Maas

TABLE OF CONTENTS

ACKNOWLEDGMENTS iii

LIST OF FIGURES viii

LIST OF ABBREVIATIONS ix

ABSTRACT xi

CHAPTER ONE: INTRODUCTION 1
Rhodium 5
CO and Rhodium 8

CHAPTER TWO: INSTRUMENTATION 10
Infrared Spectroscopy 10
Temperature Programmed Desorption 14
Low Energy Electron Diffraction 15

CHAPTER THREE: TEMPERATURE-RESOLVED SURFACE INFRARED SPECTROSCOPY OF CO ON RH (111) AND (2×1)-O/RH (111) 17
Introduction 17
Experiment 20
Results and Discussion 22
Summary and Conclusion 28

CHAPTER FOUR: CONCLUSION AND FUTURE DIRECTIONS 29

REFERENCE LIST 31

VITA 39

LIST OF FIGURES

Figure 1. Face centered cubic crystal structure 5

Figure 2. Unit cell examples 6

Figure 3. O/Rh (111) adlayer unit cells 6

Figure 4. RhO_2 model 7

Figure 5. Adsorption sites 8

Figure 6. O/CO adlayer unit cell 9

Figure 7. Beam path of IR beam through UHV chamber 11

Figure 8. Dipole moment of molecules on a metal surface 12

Figure 9. Temperature programed desorption schematic 15

Figure 10. Real space and reciprocal space lattices 16

Figure 11. CO coverage study 23

Figure 12. RAIRS results of CO/Rh (111) environment 25

Figure 13. RAIRS results of CO on (2 x 1)-O/Rh (111) environment 26

Figure 14. IR spectra and IR heat map of CO/Rh (111) and CO on (2 x 1)-O/Rh (111) environments 27

LIST OF ABBREVIATIONS

AO	Atomic oxygen
Ar	Argon
CO	Carbon monoxide
CO_2	Carbon dioxide
cm^{-1}	Wavenumber
fcc	face centered cubic
IR	Infrared spectrometer
Ir	Iridium
K	Kelvin
L	Langmuir
LEED	Low energy electron diffraction
MAES	Meitner Auger Electron Spectroscopy
ML	Monolayer
O_2	Molecular oxygen
T_{exp}	Temperature exposure
O_{ad}	Adsorbed oxygen
O_{res}	Residual oxygen
O_{sub}	Subsurface oxygen
QMS	Quadrupole mass spectrometer

RAIRS	Reflection adsorption infrared spectroscopy
Rh	Rhodium
RhO_2	Rhodium surface oxide
sec	seconds
S_0	Sticking probability
STM	Scanning tunneling microscopy
T_{dep}	Deposition temperature
T_s	Surface temperature
TPD	Temperature program desorption
UHV	Ultra-high vacuum
UHV-STM	Ultra-high vacuum scanning tunneling microscopy
θ_{CO}	Carbon monoxide coverage
θ_O	Oxygen coverage
$\theta_{O,ad}$	Surface oxygen coverage

ABSTRACT

Reflection Absorption Infrared Spectroscopy (RAIRS) is a powerful technique for identification of small molecules adsorbed to metal surfaces. Through the addition of a RAIRS system to an ultra-high vacuum (UHV) chamber, this provides a non-destructive and highly sensitive surface analysis technique. Because IR measurements can be performed in UHV conditions, interference from atmospheric species are avoided, while enabling investigation of catalytic systems. To determine the reactivity of the various oxide phases, the oxidation reaction of carbon monoxide (CO) to carbon dioxide (CO_2) on oxidized rhodium (Rh) (111) will be utilized as a probe reaction. We will be able to determine the chemical significance of various oxygen phases on different Rh surfaces, and the CO coverage and binding sites on the different oxygenaceous phases. Studying CO oxidation on different Rh surfaces will provide atomic level information regarding oxidation reactions, progressing the understanding of various surface phases relevant to many Rh catalyzed processes. Past exposure conditions determined that at low temperatures, CO was observed to adsorb along (2x1)-O and RhO_2 domain boundaries, and subsurface oxygen (Osub) replenished the reacted oxygen at these boundaries at higher temperatures. When CO was prolonged exposure, it consumed all Osub and reacted with oxides at the defects. In recent studies, it was determined that there are multiple reaction pathways available for CO oxidation, but at temperatures at or below 350 K reaction sites are not regenerate. Via RAIRS, these and other reaction sites of CO oxidation will be investigated to determine reaction pathways or mechanisms. Studying CO oxidation on different Rh surfaces

will provide atomic level information regarding oxidation reactions, progressing the understanding of various surface phases relevant to many Rh catalyzed processes. Methods developed for Rh can also be applied to other metal surfaces and small molecules of interest.

CHAPTER ONE

INTRODUCTION

Heterogeneous catalysis is a powerful technique for transformation of materials on the largest of industrial scales. In heterogeneously catalyzed reactions, the catalyst is in a different phase than the reactants; typically the reactants are in the gas or liquid phase, the catalyst is in the solid phase, and the reactions occur at the interface between the phases.[1,2] The catalyst lowers reaction energy barriers, and is regenerated over the course of the reaction.[2] Proper selection of catalysts and reaction conditions enable the acceleration of a selected reaction pathway, resulting in an increase in the selectivity for a chosen product. Ideally, undesired side reactions are hindered by application of the catalyst.[2] Gas-solid interactions are of particular interest because having the catalysts deposited on or into the surface allows the catalyst to be immobilized, therefore it can be easily recovered from the reaction. The role of surfaces in heterogeneous catalysts depends on the atoms, arrangements, and bonding properties of the metal and the gaseous or liquid-phase species.[2]

The development of heterogeneous catalysis and the application into industry practices has had a tremendous impact in many aspects of the world. One of the most important and well-known catalytic processes is the Haber-Bosch process, a method for industrial ammonia production. It was first developed in 1909 by Fritz Haber and then commercialized in 1913 by Carl Bosch. This process converts atmospheric nitrogen to ammonia by reaction with hydrogen over

an iron (Fe) metal catalyst under elevated temperature and pressures. In the gas phase this reaction is impossibly slow due to the relatively high dissociation energy of nitrogen (N_2) of ~ 900 kJ/mol. With the introduction of the Fe metal catalysis the dissociation rate decreases to ~ 80 kJ/mol.[3] Dr. Gerthard Ertl was awarded the Nobel prize for chemistry in 2007 for, among other achievements, determination of the reaction mechanism for the ammonia synthesis reaction.[3] He determined that the first step, where N_2 dissociates into two separate nitrogen atoms on the iron surface, was the rate-limiting step. Next, the individual nitrogen atoms react with co-adsorbed hydrogen atoms, then the newly formed NH_3 desorbs from the Fe surface. The development of the Haber-Bosch reaction is thought to be one of the most important inventions in the 20th century, and the world produces over 130 million tons of ammonia per year, without this reaction almost two-fifths of the world's population would not be here. [4]

To study reactive metal surfaces relevant to heterogeneous catalysis, experimentation needs to be done under ultrahigh vacuum (UHV) conditions because of the highly reactive nature of the metal surfaces. UHV pressures range from 12 to 13 orders of magnitude below atmospheric pressure (10^{-9} – 10^{-12} torr) and are generated using appropriate pumps to remove the atmosphere from a stainless-steel chamber. The removal of gases from the chamber is achieved mostly through the use of mechanical rough pumps, turbomolecular pumps and ion pumps.[5] In the low-pressure environment, gas molecules can be precisely admitted to the chamber and the interactions between the molecules of interest and the catalytically relevant surface present can be carefully, and quantitatively, studied. Understanding heterogeneously catalyzed reactions at the atomic level is very complex and these reactions usually require high temperatures and pressures. The differences between UHV reaction conditions and ambient or industry conditions are

often known as the pressure gap and bridging this pressure gap has been a prominent focus of study for many years.[6–8] In order to bridge these gaps, operando and high-pressure reaction cell experiments have been some of the methods used, offering insight to active sites of a catalyst under different reaction conditions.[9,10] While it is advantageous to investigate these reactions in these conditions, it is also advantageous to study these catalysts and reactions under UHV conditions to facilitate atomic scale understanding, and detailed chemical and structural characterization at the molecular level. [10,11] UHV conditions also allow the surfaces to remain in a prepared state for extended times, allowing for the use of highly sensitive analysis techniques involving energetic electrons. Electrons interact strongly with matter, and their mean-free-path decreases rapidly with increasing pressure.[12] Under UHV conditions, inadvertent collisions with gas molecules are unlikely, so the path and energy of the electron is dependent only on the interaction with the surface. These sensitive surface techniques can be used to characterize, quantify, and identify adsorbates. [6–89,10,11]

Studying different oxygenaceous species on metal surfaces used in heterogeneous catalysis can aid in the understanding of the oxidative catalysis at a molecular level. The interactions between oxygen and the catalytic metal differ based on the type of oxygen species present and type of transition metal. When oxygen binds to a metal surface, the adsorbate minimizes the repulsive and maximizes the attractive forces and site-dependent adsorption energy to form the most thermodynamically favored surface structure.[12–14] When oxygen molecules (O_2) are interacting with a metal surface, as the molecule approaches the surface it creates a very weak bond and physisorbs to the surface at low temperatures. As O_2 gets closer to the surface the bond becomes stronger and eventually the O_2 molecule dissociates into its individual oxygen atoms or

adsorbed oxygen (O_{ad}) which are chemisorbed to the metal surface.[15,16] Strong bonds can form between O_{ad} and the metal surface which can result in a rearrangement of metal atoms to accommodate the new oxygen atoms into the surface; these rearrangements are known as surface reconstructions.[1] Surface reconstructions can vary in how much rearrangement occurs based on the kind of metal surface. Different metal surfaces will interact with oxygen differently and it is the balance of repulsive and attractive forces between the metal and oxygen that determines how much reconstruction occurs. For example, when O_2 interacts with a silver (Ag) metal surface, large reconstructions can occur because Ag has weaker bonds between Ag atoms, so when oxygen is present, it physically rearranges the Ag atoms to accommodate the new oxygen atoms.[17,18] If a rhodium (Rh) metal surface is exposed to O_2, the dispositively adsorbed oxygen atoms create an adlayer of molecules on the Rh surface and there is no surface reconstruction.[19] Strong intermolecular interactions between O_{ad} and the metal substrate may result in the metal lattice undergoing surface reconstructions, therefore when oxygen induces surface reconstructions they can be referred to as surface oxides.[1,20,21] Oxygen-induced surface reconstructions have been extensively studied to determine how oxygen coverage of oxygen (θ_O) affect surface structure,[1,9,20,22] affect the reactivity,[9,20,23–25] and acts as an oxygen source during surface reactions.[21,26,27]

This work focuses on integrating a new spectroscopy technique to the UHV system described in the next chapter. The integration of infrared spectrometry to the system will allow a non-destructive analysis technique to be used to assist in the characterization of these oxygenated surfaces. Some techniques utilized in this dissertation are, but not limited to, Meitner-Auger electron spectroscopy (MAES), quadrupole mass spectroscopy (QMS), temperature programmed

desorption (TPD), scanning tunneling microscopy (STM), low energy electron diffraction (LEED), and reflection absorption infrared spectroscopy (RAIRS).

Rhodium

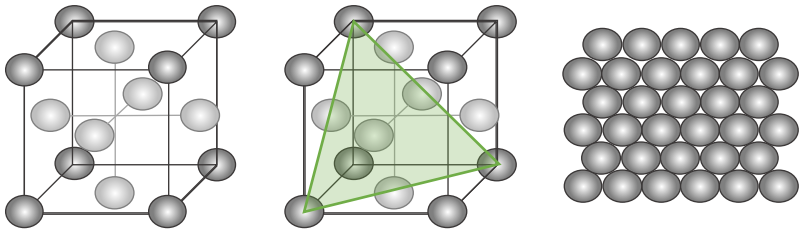

Figure 1. Left) Face centered cubic (fcc) unit cell; Center) (111) plane in the unit cell is highlighted green; Right) Representation of Rh (111) surface structure.

Rhodium (Rh) is a precious metal and is commonly used in a variety of applications, most commonly catalytic applications.[28] As a catalytic metal, Rh has been used to study reactions like the oxidation of carbon monoxide,[29] the oxidation of methanol,[30] and many more. Catalytic metal surfaces are extremely influenced by the surface structures and types of chemical species present and because of that there have been multiple studies to investigate the fundamental adsorbate-surface interactions under UHV conditions.[13,31–34] Rh has a face centered cubic crystal structure (fcc) as detailed in Figure 1. When metal single crystals are manufactured, the cut of the bulk crystals is very important, most commonly these crystals can be cut along certain axis of the crystal unit cell, providing a specific orientation of surface atoms; the nomenclature denoting how the crystal was cleaved is known as a Miller index.[2,35] Using a Rh (111) surface is a common crystal orientation used in many types of studies.[15,29,36–38] For a (111) orientation, the crystal is cut so that the surface plane intersects the x, y, and z axes at the same value (Figure 1, center) which creates a flat surface of hexagonally close packed (hcp) atoms (Figure 1, right).

Along with Miller indices, another commonly used descriptive tool is Wood's notation, which describes the adsorbate surface structure in relation to the metallic lattice.

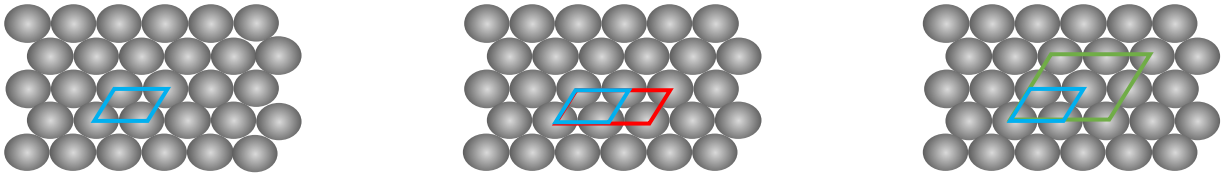

Figure 2. Examples of unit cells on a Rh(111) surface. Left) (1×1) unit cell in blue; Center) (2×1) unit cell in red; Right) (2×2) unit cell in green.

Unit cells are defined as the smallest possible repeating unit of surface, typically shown as vectors drawn on the surface image as seen in Figure 2. The unit cell for a fcc (111) system is a (1 × 1) unit cell and surface adlayers are identified compared to the native (1 × 1) unit cell. A (2 × 1) adlayer unit cell is two atoms long along one side of the unit cell and one atom long on the other (Figure 2, center). If the unit cell is rotated with respect to the native unit cell, it is noted by R and the angle of orientation. The unit cell of an adsorbed layer that is twice the size of the native (1 × 1) would be noted as a (2 × 2).

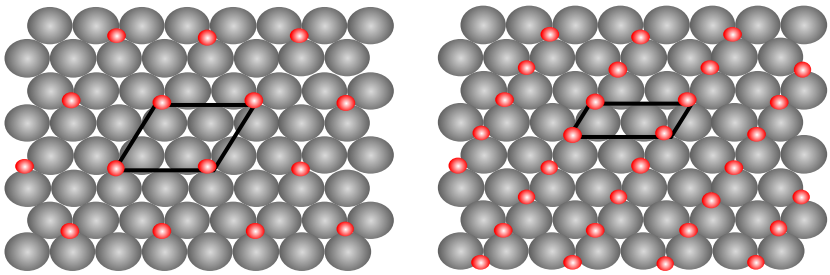

Figure 3. Surface models of O/Rh (111) surface structures, with Rhodium atoms grey and Oxygen atoms red. Left) (2 × 2) unit cell, Right) (2×1) unit cell.

When O_2 molecules interact with Rh (111) surfaces, O_2 dissociates into the individual oxygen atoms (O_{ad}). Partial oxidation of Rh (111) upon exposure to O_2 results in the formation of a (2 × 2)-O adlayer equivalent to 0.25 monolayer (ML) O coverage as determined via LEED, shown

in the left of Figure 3.[34,39] When O_2 exposures are increased, the surface saturates at 0.5 ML O coverage. It was determined via STM that the surface was dominated by (2 × 1)-O domains (Figure 3, right), which corresponds to a surface saturation where kinetic constraints of O_2 dissociation have been reached.[5,15,40–42] In order to reach higher coverages, $\theta_O > 0.5$ ML, a different oxygen source needs to be utilized.

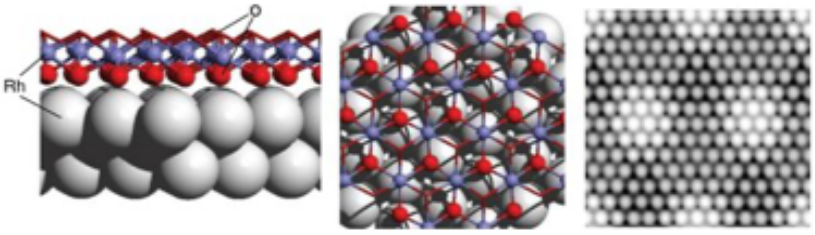

Figure 4. RhO_2 oxide model on Rh(111) Left) side view; Center) top view; Right) simulated STM.[12]

Oxidation of the Rh surface with atomic oxygen (AO) allows $\theta_O > 0.5$ML under UHV conditions, with the formation of subsurface oxygen (O_{sub}) at elevated substrate temperatures. O_{sub} is observed desorbing from Rh (111) in a single sharp desorption features at ~ 800 K during TPD experiments. [5,43] While AO exposures can form the (2 x 1)-O adlayer and O_{sub}, it also can form oxides along step edges and defect sites at elevated substrate temperatures.[19,33,44] The main oxide that forms and that has been extensively characterized is RhO_2, displaying a single layer stacking structure of O-Rh-O.[12,45] It has been determined that the oxide has metallic behavior, and is thermodynamically stable.[45] When RhO_2 is investigated via STM, the RhO_2 appears as a Moiré pattern (Figure 4, right), where the (8 × 8) Rh substrate with a 2.69 Å lattice which is below a (7 × 7) RhO_2 surface with a 3.02 Å lattice.[5,15,20,21,45] The slight mismatch between the lattices causes the Moiré pattern.[5,12,43] This reconstruction layering is seen to have a layer of Rh atoms between two layers of O atoms.

CO and Rhodium

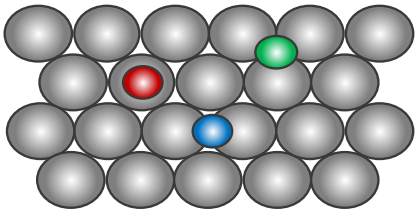

Figure 5. Model of different adsorption site. Red: atop site, Blue: bridge site, Green: hollow site

CO is a common molecular adsorbate used to probe surfaces to better understand surface structure and reactivity. The oxidation of CO to CO_2 is a benchmark surface reaction because of the simplicity.[48] Depending on the surface, CO can provide a variety of surface behaviors and is a prototypical molecule to study using various methods and techniques. CO does not dissociate on Rh(111) and chemisorbs as an intact molecule. CO can bind to different surface sites as coverage increases, and when in the presence of oxygen, the adsorption behavior and structures are more complicated (Figure 5). It favorably adsorbs to the atop (red) sites and arranges in a $(\sqrt{3} \times \sqrt{3})R30°$-CO adlayer with θ_{CO} of 0.33 ML. At higher θ_{CO}, CO will also adsorb to bridge (blue) sites and forms a (2×2)-3CO structure adlayer.[13,31,49–51] When O_{ad} and CO are co-dosed onto the Rh (111) surface, it forms a (2×2)-2O+CO adlayer (Figure 6), and CO binds on the atop sites.[50,52] Some of the recent work in the Killelea lab has focused on CO oxidation on Rh (111) with a mix of oxygenated species present, mainly the types discussed above, O_{ad}, O_{sub}, and RhO_2. With $\theta_O > 0.5$ ML, with AO and O_{sub} present, it was shown that surface and subsurface oxygen was rapidly consumed at modest temperature CO oxidation.[29] STM images showed that prolonged CO exposures consumed O_{ad}, reacted most of the O_{sub} and oxides along the defect sites, and that O_{sub} was not able to replenish the oxygen depleted sites.[29] When observing CO oxidation of O_{ad}, $\theta_O \leq 0.5$ ML and the effect of surface temperature it was determined that surface temperature had little effect

on oxidation. It was determined that only a fraction of O_{ad} was used in the oxidation and that at low temperatures reactive species were not replenished.[53] Under high oxidation condition when oxides form, it has been observed that CO does not adsorb readily on the oxide directly, but rather on oxide defects and metallic patches on the surface.[46] RhO_2 oxides have been shown to have high production of carbon dioxide (CO_2) when present and is thought to be very catalytically active and important to catalytic function.[9,45,47]

This dissertation work focuses on monitoring the CO oxidation on various oxygenated Rh (111) surfaces via RAIRS spectroscopy. This new surface technique to this chamber allows for a unique perspective and investigates these reactions. The main goal is to quantify the coverage of CO present on oxygenated surfaces and determine the adsorption and reaction sites in these environments. With the addition of this information, the goal is to better understand the CO oxidation and oxygenated surfaces from past studies.

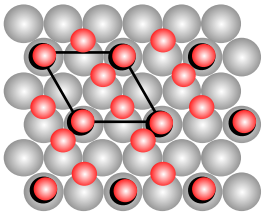

Figure 6. Model of co-adsorbed O and CO species on Rh(111). Adlayer forms a (2 × 2)-2O + CO unit cell.

CHAPTER TWO

INSTRUMENTATION

UHV surface science techniques require ultra-high vacuum, with pressures as low as 1 x 10^{-12} torr for experimentation to be performed. In order to fully elucidate the interactions between gas phase reactants, condensed phase species, and the catalytically active substrate, a combination of analysis tools are needed. The following techniques were used to collect the data presented herein: reflection absorption infrared spectroscopy (RAIRS), temperature programmed desorption (TPD) or temperature programmed reaction (TPR), low electron energy diffraction (LEED), and scanning tunneling microscopy (STM). Further information about techniques not mentioned below can be found in Derouin, et al.[5] Surface techniques mentioned below have specific impact on the research shown in this dissertation or have been newly integrated to the chamber as part of this dissertation work.

Reflection Absorption Infrared Spectroscopy

Infrared spectroscopy is the measurement of infrared light as it interacts with matter via vibrational-rotational transitions. When infrared light interacts with a sample, it can be affected in different ways mainly by absorption, emission, or reflection. The resulting infrared light can then be measured and used to determine chemical species, functional groups, etc depending on the ex-periential set up. Specifically, RAIRS is a powerful, surface sensitive, nondestructive technique for identification of small molecules adsorbed to metal surfaces.[54] Because IR measurements can

be performed under UHV conditions, interference from atmospheric species are avoided, thus enabling the investigation of catalytic systems. IR spectroscopy with experiments involving high resolution, polarization, time resolution, or high pressures[55] has been used to determine the orientation and structure of surface adsorbates,[54,56] determination of increasing coverages,[56,57] to aid in the determination of precursors,[57] but also to monitor the reactions as experimental conditions vary,[57–59] or to track reactions through time points.[58,59]

The use of IR spectroscopy to study adsorbates on a surface dates back to the 1940s but the application of this technique to characterize adsorbates on metal surfaces did not become common until the 1950/1960s.[54,60] In the mid 1960s, Greenler observed that sub-monolayer concentrations of adsorbates on bulk metals could be determined at grazing angles, thus this approach of reflection absorption infrared spectroscopy (RAIRS) allowed for information about chemical identity, geometry and adsorption sites to be investigated on the surface.[61] At the beginning, the C-O vibrational stretch on copper films was investigated, but as the technique developed, it has been utilized to investigate much more complex systems such as nitrogen/hydrogen stretch,[62] carbon

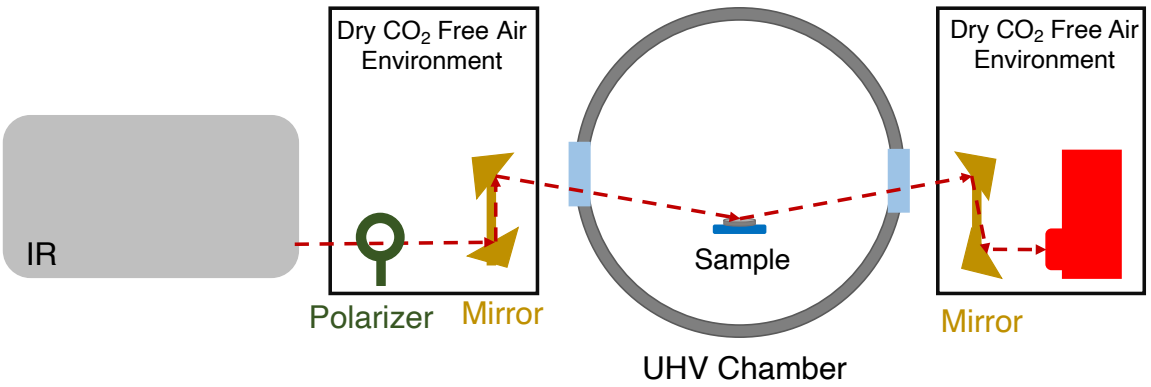

Figure 7. Beam path of infrared beam through UHV chamber. Beam is indicated by dashed red line, with components used in analysis labeled in order beam path travels through.

nanofibers,[63] or nanoclusters[64] on other metal surfaces besides Rh, e.g. platinum (Pt)[62,65,66] or more complex surfaces like single atom alloys[67,68]

The RAIRS apparatus design is extremely important and basic design components have been developed for optimal results. RAIRS utilizes an infrared beam that travels through a chamber, interacts with the sample, and the reflected signal is then collected via a detector. It is best when the beam path is as short as possible, to limit any interferences to the beam. A large part of this dissertation was spent interfacing an IR spectrometer to the existing chamber in the Killelea lab, the resulting beam path is depicted in Figure 7.

The infrared beam travels from the commercial IR spectrometer (Bruker, Invenio R) through a polarizer. The polarizer is used to increase any IR active molecules' vibrations on the surface and this increase sensitivity of these vibration stretches. The surface dipole selection rule is the most important foundation to interpret spectral data, it states that the vibrational mode will be IR active if there is a non-zero projection of dynamic dipole moment of the vibrational mode normal to the surface.[56] This means that when a molecule is adsorbed on a surface, the molecule induces an opposite image charge within the surface substrate. The dipole moment of the molecule and the image charges perpendicular to the surface reinforce each other, while parallel charges

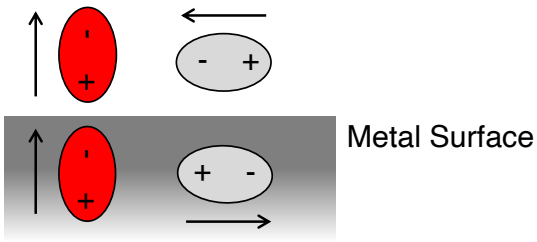

Figure 8. Visual cartoon of the dipole moment of molecules interacting with metal surface, illustrating the surface dipole selection rule.

cancel each other out (Figure 8). There are two types of polarization, s-polarization which is perpendicular to the incident plane but aids in the cancellation of parallel dipole moment and p-polarization which is parallel to the incident plane and which increases the signal of the dipole moments perpendicular to the surface.[69] Once the infrared light is polarized it then passes through a set of gold-plated mirrors to direct the beam through potassium bromide (KBr) salt windows into the UHV chamber. Salt windows are used in this situation so that the IR light can travel into the chamber, where normal windows would block the IR light. Once directed into the chamber, it interacts nondestructively with the surface and its adsorbates at a grazing incident angle. The sample and adsorbates that are present on the surface absorbs energy from the beam, then the resulting energy left in the infrared beam is directed out of the chamber. Once out of the chamber, the infrared beam is directed using another set of gold-plated mirrors into a liquid nitrogen–cooled mercury cadmium telluride detector. The use of a liquid nitrogen cool detector allows for increased sensitivity.

CO is a common molecular adsorbate used to probe surfaces to better understand surface structure and reactivity. Depending on the surface, CO can provide a variety and diverse types of surface behaviors and is a prototypical molecule to study using various methods and techniques. In general, metal to the left of the periodic table dissociate CO into separate atoms and bind to hollow sites of the surface.[59] For metal on the right on the periodic table, CO remains intact when exposed to the surface and binds via the carbon atom.[59] The CO axis is perpendicular to the surface, and adsorption sites vary depending on the surface structure.[59] In the case of Rh(111), atop sites are preferred at low coverages, but for higher coverages more than one surface site is occupied.[12] The oxidation of CO to CO_2 is a

benchmark surface reaction because of the simplicity.[56,14] There have been two mechanisms of CO oxidation observed. In an associative mechanism, the CO reacts with surface bound O_2; while a dissociative mechanism where O_2 dissociates first onto the surface and then O_{ad} reacts with CO to form CO_2. The latter is the mechanism studies through these experiments. To monitor and track CO oxidation, RAIRS can be utilized because CO strongly absorbs IR light, so monitoring the C-O stretch can yield valuable information. CO has been used to qualitatively probe the state of the surface through the sensitivity of the main CO stretch frequency to metals and to different binding sites.[57,67,14,70,71] When CO is bound to Rh(111), the stretch for the CO in atop sites has an absorption peak calculated and observed between 2015 cm^{-1} and 2100 cm^{-1}, depending on surface CO coverage.[49,72] When CO coverages are high enough, CO can also bind at the bridging sites which has been observed and measured at 1851 cm^{-1} to 1861 cm^{-1}.[49,73,52,74] When the surface is oxygenated first, CO remains bound in atop positions (observed around 2085 cm^{-1}) while oxygen atoms are located in the hollow sites.[49] Because oxygen is present, CO has less adsorption spots available, so CO tends to bind only at the atop sites, not the bridging sites.

Temperature Programmed Desorption

Temperature programed desorption (TPD) is a useful surface technique that utilizes mass spectrometry to determine the quantity and identity of the chemical species desorbing from the metal crystal surface as temperature is linearly ramped up. The mass spectrometer mass-to-charge ratios and fragmentation patterns are used to aid in the identification of desorbing molecules and atoms. At the start of a TPD experiment, the temperature of the crystal is typically at 300 K when running oxygen experiments, and 100 K when running CO

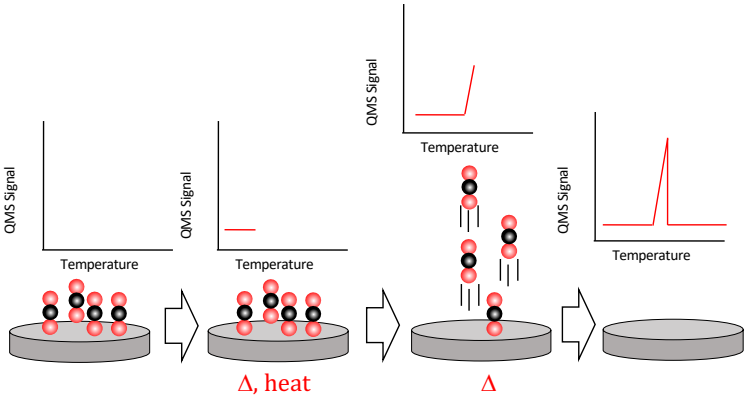

Figure 9. Cartoon schematic of TPD events. From left to right, temperature of the sample is increased, resulting in molecules desorbing from the surface. The resulting trace of molecules is determined via mass spectrometry mass-to-charge ratios.

experiments. The temperature is then linearly ramped to the maximum temperature programmed. It is important that the temperature ramp is as linear as possible to avoid unwanted pressure spikes from the desorbing species. As temperature of the sample increases, the energy of the sample also increases, which increases the probability that the adsorbate will desorb from the surface and the resulting trace from the desorbing species are analyzed (Figure 9).[75,76]

Low Energy Electron Diffraction

Low electron diffraction (LEED) is a useful technique to determine the long-range surface structure. Electron diffraction was experimentally proven through the Davisson and Germer experiment which proved that electrons have wave behavior, confirming the deBrogile hypothesis that all matter exhibits wave like properties.[77] The experiment was able to prove that electrons showed diffraction patterns, by firing low energy electrons at a nickel crystal surface and observing angular dependence of intensities of scattered electron beam. The peaks indicated the wave behavior of the electrons and when interpreted through Bragg's law indicated the lattice spacing of the

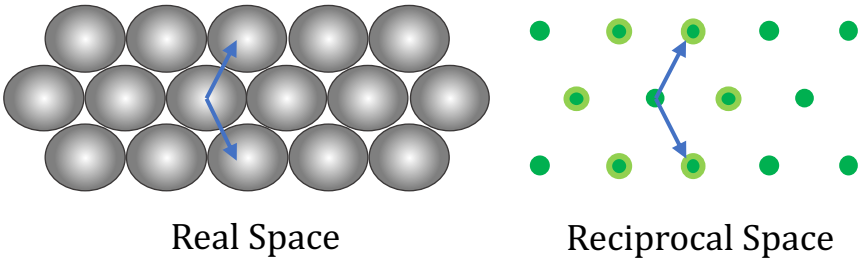

Figure 10. Real space and reciprocal space lattices of a (111) surface.

nickel crystal. This technique works by applying a beam of monoenergetic electrons with modest energy (10-1000 eV) from an electron gun directed towards the sample surface. These electrons interact with the surface and diffract away from it towards a phosphor-covered screen. There are 2-4 wire mesh screens in front of the phosphor screen, and the potential of each can be varied to provide a high-pass filter that discriminates non-diffracted electrons and allows only the higher energy electrons to pass through. Where the electrons hit the phosphor screen, light is emitted, and the diffraction pattern is evident in the spots on the screen. The diffraction pattern that is observed is the reciprocal lattice of the surface structure (Figure 10). The reciprocal lattice is a direct reflection of the crystal's surface (Figure 10). Comparing LEED patterns before and after exposures can be very useful to determine surface changes and track progression of change,[78,33] or monitoring the growth of thin films.[79]

CHAPTER THREE

TEMPERATURE-RESOLVED SURFACE INFRARED SPECTROSCOPY OF CO ON RH (111) AND (2 x 1)-O/RH (111)

Reprinted with permission from **Temperature-Resolved Surface Infrared Spectroscopy of CO on Rh(111) and (2x1)-O/Rh(111)**, Elizabeth A. Jamka, Maxwell Z. Gillum, Christina N. Grytsyshyn-Giger, Faith J. Lewis, and Daniel R. Killelea, *Jounral of Vacuum Science and Techonolgy A* **2022** *40* (4), 043209. Copyright 2022 American Vacuum Society

CO oxidation over transition metal surfaces provides insight into the relative reactivity of various surface phases. Surface IR spectroscopy is a quantitative technique that also provides information about the binding sites and chemical environments of the adsorbed CO molecules. Here, we report results from a study of CO sticking to clean Rh (111) and (2 x 1)-O/Rh (111) that shows that the intensity of the IR absorption was not linear with coverage and is an important consideration for further study of catalytic surface.

Introduction

The oxidation of small molecules over metal surfaces is of widespread importance in heterogeneous catalysis.[80,20,81] In particular, the oxidation of carbon monoxide (CO) to carbon dioxide (CO2) has attracted much interest because it is relevant to industrial and consumer processes (e.g., catalytic converter in automobiles) and also because it allows for the study of the surface

species because of the lack of molecular complexity.[31, 48] CO oxidation has been studied using a variety of techniques including molecular beam – surface reactive scattering,[82,83,84] temperature programmed desorption/reaction (TPD/TPR) to monitor the production of CO_2,[53,29,85,86,87] X-ray Photoelectron Spectroscopy (XPS) to speciate the surface species through the reaction via elemental analysis, and Reflection-Absorption Infrared Spectroscopy (RAIRS), which provides molecular information about the surface adsorbates.[24,88,49,89] Together, a picture has emerged about the surface-catalyzed oxidation of CO on a variety of different metal surfaces, but as key details are discovered, there is an emerging consensus that this seemingly 'simple' reaction is far more complicated than was thought even a few years ago.[83, 90, 91] In particular, recent discoveries showing that surface oxide reactivity is strongly correlated to geometry[92] and that terrace and steps proffer very different catalytic activities,[83, 22] has spurred us to study the different oxygenaceous phases on Rh (111), where we have developed robust approaches for preparing three distinct phases.[37,33,5] Here, we present results showing that even CO adsorption to clean Rh (111) has complexities that must be considered in order to properly use RAIRS to determine the species present and their coverages.

The IR absorption spectrum of adsorbed CO is sensitive to the binding site and thus has been used to qualitatively probe the state of the surface through the sensitivity of the main CO stretch frequency to metals.[71, 67] Although CO spectroscopy is well-developed, there have been only a handful of IR studies of CO on Rh (111) [49, 72, 51] and even fewer investigating CO on oxygenated Rh (111) surfaces.[49, 50] We have determined the chemical significance of various oxygen phases on different Rh surfaces,[53, 29, 37,33,5] and here, we have studied CO adsorption on Rh (111) and (2 × 1)-O/Rh (111). Studying CO oxidation on different Rh surfaces provides atomic level

information regarding oxidation reactions, progressing the understanding of various surface phases relevant to many Rh catalyzed processes.

O_2 readily dissociates on Rh(111) to form adsorbed oxygen (O_{ad}), and adsorption is kinetically limited to an oxygen coverage (θ_O) of 0.5 monolayers (ML, 1 ML = 1.6×10^{15} atoms cm^{-2}).[53, 93, 13] CO does not dissociate on Rh (111) and chemisorbs as an intact molecule. CO preferentially adsorbs on atop sites and arranges in a ($\sqrt{3}$ x $\sqrt{3}$)R30°-CO adlayer with a CO coverage (θ_{CO}) of 0.33 ML CO. Upon continued exposure, CO adsorbs to bridge sites as well and reaches θ_{CO} = 0.75 ML in a (2 x 2)-3CO structure.[31, 49, 94] The CO stretch for CO in atop sites has an absorption peak calculated and observed between 2015 cm^{-1} and 2100 cm^{-1}, depending on θ_{CO}.[49, 72] On oxygenated surfaces, CO remains bound atop, while O occupies the hollow sites,[49] and the CO stretch was observed to increase by ≈ 25 cm^{-1} to 2085 cm^{-1}.[49] However, it is important to note, that the previous IR measurements were typically made at low-temperature (T_{exp} < 200 K) and it does not seem that the behavior of the IR spectra with respect to temperature has been investigated.

In this paper, RAIRS and TPD were employed simultaneously to determine both the CO coverage on the surface and the binding sites and chemical environment for CO on Rh (111). The combination of TPD and RAIRS provides the chemical species and their local environment over a range of surface temperatures and adsorbate coverages. With the behavior of CO on clean Rh (111) established, the adsorption of CO to an oxygenated Rh (111) surface, the (2 × 1)-O structure, was studied over a range of temperatures during a TPD experiment. In both cases, we observed that the IR peak shifts in accordance with previous measurements, but the intensity varies and is most intense, on a per-molecule basis, at low coverages. This suggests that the intensi-

ty of the absorption for the CO stretch does not linearly depend on θ_{CO}, meaning that correlation of θ_{CO} to the RAIRS signal requires more than a simple application of Beers Law to the IR spectra.

Experiment

All experiments were performed in an ultra-high vacuum (UHV) system described previously.[5] The system is comprised of two connected chambers, a preparation chamber (base pressure of 1×10^{-10} Torr) and a scanning tunneling microscope (STM) chamber (base pressure of $<2 \times 10^{-11}$ Torr). The preparation chamber was equipped with multiple surface science techniques including a Specs ErLEED 150 with 3000D controller (LEED), a PHI 10-155 Meitner-Auger Electron Spectrometer (MAES), and a Hiden HAL 3F 301 RC quadrupole mass spectrometer (QMS) for temperature programmed desorption (TPD) analysis. RAIRS measurements were made with a Bruker FT-IR Invenio R spectrometer and an external liquid nitrogen cooled MCT (mercury-cadmium-telluride) detector which increased sensitivity to around 800 cm^{-1}. The IR light was p-polarized and traveled through enclosures purged with dry, CO_2 free air (Parker, Spectra30, FT-IR Purge Gas Generator). The RAIRS spectra are an average of 36 scans were taken with a resolution of 4 cm^{-1} and new background spectra was taken at the start of each experiment. In some of the spectra on Rh (111), a small spurious background absorption peak, likely from adsorbed CO from the chamber background, was present when the IR background was obtained. This resulted in a negative peak in the $\Delta R/R$ or absorbance spectra around 2025 cm^{-1} that appeared after CO exposure began and remained even after CO was desorbed. The small intensity and far-red shift indicated that this was only a small amount of CO. When present, this was removed from the spectra by taking CO stretch portion of the spectrum at high temperature,

where the surface was clear of CO, inverting it, and adding it to all the spectra collected in that trial. This peak was never observed on the oxidized surface.

The Rh (111) crystal (Surface Preparation Labs, Zaandam, The Netherlands) sample was a 10 mm diameter disc and 3 mm thick and was mounted on an exchangeable tantalum (Ta) sample plate with a type-K thermocouple welded to the side of the crystal. The crystal could be cooled with liquid nitrogen loop to 100 K and heated using electron beam heating to 1400 K. The surface was cleaned with repeated cycles of Ar^+ sputtering and annealing at 1300 K until the surface cleanliness was verified with a clean (1 × 1) LEED pattern and O_2 TPD free of CO_2.

The Rh (111) sample was dosed with CO with a pressure of 1×10^{-6} Torr at an exposure temperature (T_{exp}) of 300 K. For the oxidized surface, the Rh(111) was first dosed with O_2 by backfilling to 1×10^{-6} Torr for 60 sec at T_{exp} = 300 K to yield a saturated surface with the adsorbed O (O_{ad}) in a (2x1)-O adlayer and θ_O = 0.5 monolayers (ML, 1 ML = 1.6×10^{15} atoms cm^{-2}).[53] After oxygen preparation, the surface was then separately dosed with CO at 1×10^{-6} Torr at T_{exp} = 300 K. Spectra were obtained both during CO exposure to measure uptake and during the TPD experiment to complement the QMS desorption measurements. Spectra between 850 and 4000 cm^{-1} with a resolution of 4 cm^{-1} were collected every 10 sec. For the TPD experiments, QMS and RAIRS spectra were collected synchronously. The TPD was run from 100 K to 600 K with a ramp rate of 0.4 K sec^{-1}. CO oxidation on Rh (111) was complete by 600 K. The Rh (111) crystal was then annealed to 1250 K in between experiments to restore surface cleanliness and order, as verified with LEED.

Results and Discussion

In order to use the IR spectra to quantify θ_{CO}, it was first necessary to establish θ_{CO} as a function of CO exposure at T_{exp} = 300 K. Figure 11A shows the TPD spectra taken after several CO exposures, clearly demonstrating the surface saturation after ≈ 15 Langmuir (L) CO exposure. The TPD spectra were background subtracted (as shown in Figure 11A) and then integrated to obtain θ_{CO} using the known saturation coverage of CO on Rh (111) of θ_{CO} = 0.75 ML CO,[94] the CO uptake is shown in Figure 12B with the integrated TPD desorption in red on the left and the calculated θ_{CO} in blue on the left plotted with respect to the CO exposure in L.

With the uptake quantified, the correlation between the RAIRS and θ_{CO} could be determined. Figure 12A shows RAIRS obtained after each of the CO exposures at T_{exp} = 300 K, in Figure 11A. Curiously, the highest peak was observed at 2072.2 cm^{-1} after a 1 L CO exposure, θ_{CO} = 0.19 ML, and continued exposure saw the peak steadily redshift to 2084.2 cm^{-1}, broaden slightly, and diminish in amplitude. As coverage was determined from the TPD spectra, it is not the case that CO was desorbing at 300 K for the longer CO exposures. Instead, it is more likely that the increased coverage decreased the per-molecule IR absorption cross-section as the electron density available from the metal decreased, and the C–O bond strength increased, as suggested by the blue shift in the CO stretching absorption feature. The net result is that this seemingly anomalous behavior is indicative of a shift of electron density from the CO–metal bond to the CO molecule. Although this could be rationalized by ‘back-bonding’ where the metal contributed electron density to the $2\pi^*$ antibonding orbital in CO, the situation is probably more complex, but the result the same.[95,12,96] Above θ_{CO} ≈ 0.6 ML, this effect diminished and the peak intensity remained constant, while still modestly blue-shifting.

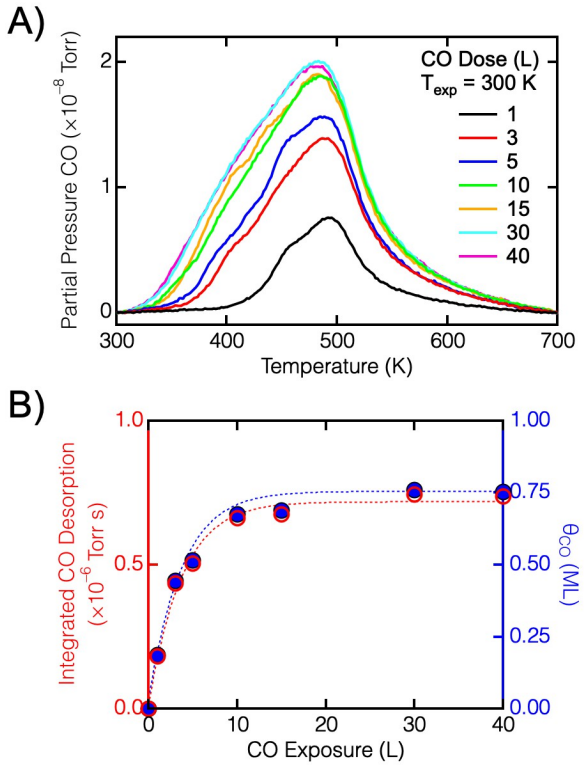

Figure 11: A) TPD spectra of m/z = 28 (CO^+) after exposing Rh (111) surface to varying amounts of CO at T_{exp} = 300 K. Initial coverages are θ_{CO} = 0.19 ML (—), 0.45 ML (—), 0.52 ML (—), 0.67 ML (—), 0.69 ML (—), 0.76 ML (—), and 0.75 ML (—). The heating rate was 4 K sec^{-1} for TPD. B) Integrated TPD area showing the uptake of CO at varying exposures and correlation between integrated desorption (red open circles, left) and θ_{CO} (blue filled circles, right).

The convoluted relationship between absorption frequency and peak intensity was also present when surface temperature (T_s) increased concomitantly with a decrease in θ_{CO}, as shown in the RAIRS collected during the TPD experiment in Figure 12B after a 30 L CO dose at T_{exp} = 300 K and $\theta_{CO,initial}$ = 0.75 ML. With increasing T_s, and thus decreasing θ_{CO}, the C–O stretch frequency red-shifted, suggesting strong CO–metal bond and weakening C–O bond, while the intensity does not appear to decrease linearly with θ_{CO}. The observation of a pronounced increase in intensity for the absorbance of the C–O stretch was robust, as it was observed with isothermal

uptake at T_{exp} = 300 K and during the TPD experiment where $T_s \approx 500$ K; the spectra for similar θ_{CO} for the two different paths is shown in Figure 12C. Although we are unable to state definitely why the absorption frequencies differ, it is reasonable to assume that the shift is caused by the difference in T_s for the two spectra. This effect is also evident in Figure 12D for a 30 L CO dose at T_{exp} = 300 K, and $\theta_{CO,I}$ = 0.75 ML, where the black trace (right axis) is θ_{CO} from the TPD measurement and the red circles (left axis) is the integrated intensity of the C–O stretch peak (between 2072 cm^{-1} and 2086 cm^{-1}) in the RAIRS data. As shown, despite a roughly 50% decrease in θ_{CO}, the integrated intensity of the CO stretch peak actually increased. With additional desorption the RAIRS signal did diminish, but at the point where θ_{CO} was down to 25% or so of the original value. It is important to note that the θ_{CO} from the TPD measurement was an upper limit, and most likely exceeded the actual θ_{CO} at any moment because the QMS was measuring the partial pressure and there was some lag due to the pumping speed for CO in the UHV chamber.

On the (2 × 1)-O adlayer at 300 K or below, CO also adsorbed intact and inserted into the adlayer forming a (2 × 2)-2O+CO adlayer.[72, 50] Although at higher temperatures CO would be oxidized, removing O_{ad}, for T_s < 300 K, the reaction was not significant.[53] RAIRS taken after exposure of (2 × 1)-O to CO is shown in Figure 13A, and only a single absorption peak, corresponding to a C–O stretching mode, was observed at 2088 cm^{-1}. Unlike CO on Rh (111), there was no shift in the peak location and the intensity monotonically increased with exposure, and rapidly saturated. This straightforward relationship between CO exposure and RAIRS intensity suggests that the factors that gave CO on Rh (111) the complex behaviors were not present on the oxygenated surface, likely because, although still metallic, O_{ad} reduced the availability of

electron density to the CO, and contributions to CO–Rh orbitals aside from the surface–adsorbate bond did not occur.

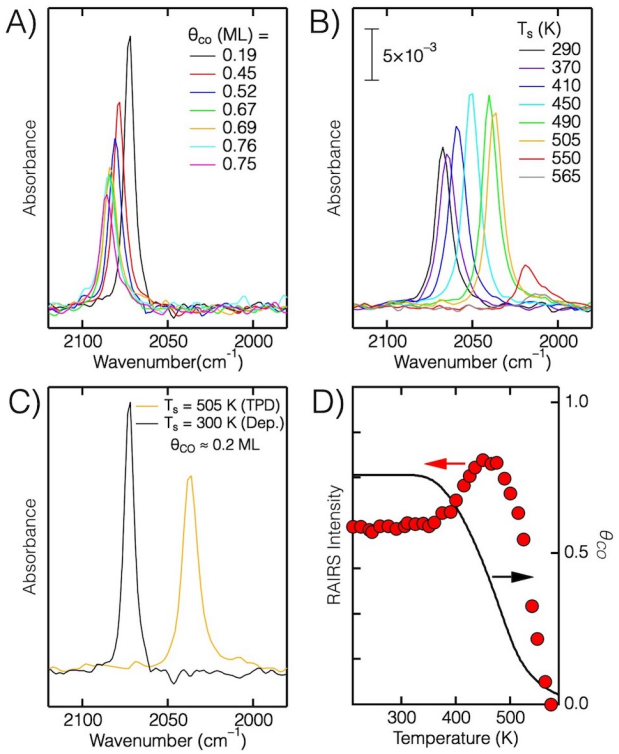

Figure 12: CO on Rh (111) A.) IR spectra of varying doses taken after the CO exposures shown in Fig. 1 at T_s = 300 K. B.) Sequence of the IR scans taken through TPD experiment with $\theta_{CO,\ initial}$ = 0.75 ML. These show the decreased intensity and red shift in the CO absorption peak as temperature increased and θ_{CO} decreased. C) The difference in IR spectra for similar coverages ($\theta_{CO} \approx$ 0.2 ML) collected after a 1 L CO dose at 300 K (—) and during the TPD experiment when θ_{CO} has deceased from 0.76 ML (—), collected at 505 K. All RAIRS plots have the same vertical range, given by scale bar in panel B). D) RAIRS intensity (left) $\theta_{CO,\ initial}$ = 0.76 ML during TPD experiment (red circles) and θ_{CO} from TPD data (right, —).

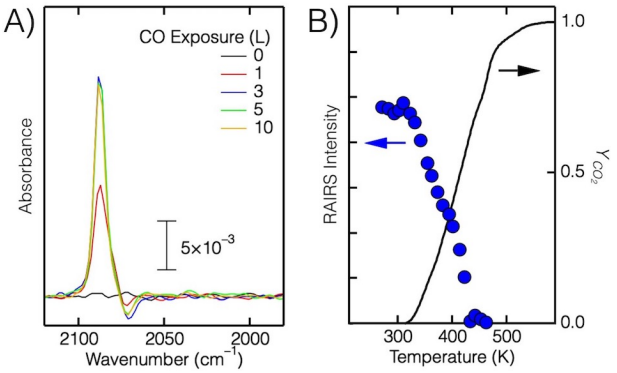

Figure 13: CO on (2 × 1)-O/Rh (111). A) RAIRS taken during CO exposure for T_{exp} = 300 K showing single C–O stretch absorption peak that rapidly saturated. B) RAIRS intensity (left) for CO on (2×1)-O during TPD experiment (blue circles) and Y_{CO} from TPD data (right), the integral of the CO_2 desorption peak.

However, IR spectra collected during the TPD experiment showed a transition does not present for CO/Rh (111). As shown in Figure 14A, and 14B around 300 K (the CO exposure temperature) the absorption peak shifted from 2088 cm^{-1} to 2068 cm^{-1}, the same frequency observed for CO on clean Rh (111). In addition, there was no absorption corresponding to CO binding at bridge sites, which was evident on Rh (111) in Figures 14C and 14D around 1850 cm^{-1}. This shift occurred at the onset of CO oxidation to CO_2, as indicated by the appearance of CO_2 in the TPD, shown in Figure 13B (right axis, black trace). After a narrow window of coexistence, only the 2068 cm^{-1} peak was observed, and then as T_s increased, the RAIRS intensity steadily decreased, as shown in Figure 13B, left axis. The fact that the shift in IR absorption and desorption of CO_2 occurred simultaneously indicated that the reactive CO fingerprint was the 2068 cm^{-1} mode. However, it is unclear at this point if this was due to a shift in binding site or from another factor. Figure 14 compares how the IR spectra of oxygenated to clean Rh (111) evolved with T_s and θ_{CO}. As previously discussed, on Rh (111), CO desorption caused an increase in the RAIRS intensity although θ_{CO} decreased, shown in Figures 14C and 14D. On the oxygenated surface, shown in Figures 14A and 14B, the RAIRS peak was unchanged until the transition

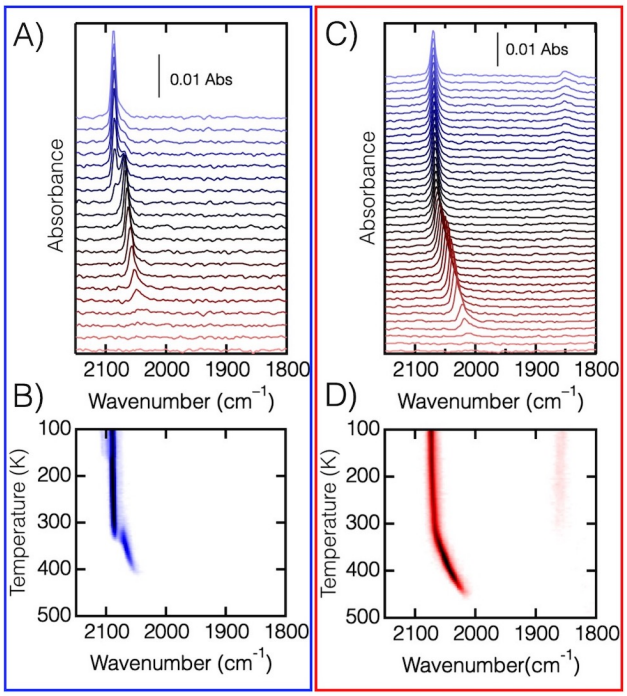

Figure 14: A) (top) IR spectra taken during TPD experiment for an initial preparation of 30 L CO exposure at T_{exp} = 300 K on (2×1)-O/Rh(111). The transition from a single peak at 2088 cm^{-1} to 2068 cm^{-1}, with a limited coexistence around 300 K. B) 2-D plot to highlight the peak shift. C) IR spectra for 0.76 ML CO on Rh(111) during TPD ramp and D) 2-D plot to highlight smooth shift in maxima.

to 2068 cm^{-1} near 300 K, and thereafter followed the same path as CO on Rh (111) without O_{ad}. However, instead of merely desorbing, the CO was being oxidized to CO_2. This suggests that CO oxidation occurred along the desorption pathway, as the chemical state was the same, as indicated by the C–O absorption peak location. However, the steady decrease in RAIRS intensity with θ_{CO} shows that RAIRS intensity was proportional to the CO coverage on the oxygenated surface.

Summary and Conclusion

The intensity and location of the C–O stretch from the surface IR spectra of CO on Rh (111) and (2 × 1)-O/Rh (111) clearly depended on the surface temperature. On clean Rh (111),

CO deposited at 300 K yielded a sharp C–O absorption peak between 2072 cm^{-1} and 2086 cm^{-1}, characteristic of adsorption on Rh atop sites, and a significantly smaller, broad peak near 1850 cm^{-1} corresponding to binding on Rh bridge sites. Upon heating in a TPD experiment, the atop C–O stretch first increased in intensity, before decreasing and redshifting as θ_{CO} decreased. Alternatively, RAIRS of CO on (2 × 1)-O/Rh (111) gave only the atop C–O stretch feature initially at 2088.5 cm^{-1}, which shifted to ≈2070 cm^{-1} with heating and the progress of CO oxidation until it too diminished in intensity and redshifted as seen on clean Rh (111). These results show that quantitative RAIRS requires more than only peak intensity. Furthermore, because the CO chemical environment was the same whether O_{ad} was present or not, CO oxidation occurs along the desorption pathway. These results show the subtle interplay between coverage and temperature for CO oxidation on rhodium surfaces.

CHAPTER FOUR

CONCLUSION AND FUTURE DIRECTIONS

A large part of this dissertation dealt with the integration of a commercial IR system to the existing UHV system in the Killelea Lab. The largest hurdles included building components for the purge gas system and aligning the IR beam to travel through the components, interact with the sample, travel into the detector with sufficient signal intensity for spectral analysis. Once the system was aligned, experimentation was able to begin starting with simple surface environments and then increasing in complexity.

This dissertation focus on the surface characterization of CO and oxygen co-adsorb on Rh (111) via simultaneous RAIRS and TPD spectroscopy. This work focuses specifically on CO/Rh (111) and (2 × 2)-2O + CO/Rh (111) surfaces. Results indicated that these environments are not as simple as originally thought. On clean Rh (111), when CO saturates the surface two peaks are observed, a sharp peak at 2072 cm^{-1} – 2086 cm^{-1} and a much broader peak around 1850 cm^{-1}. These C-O stretches correspond to the atop and bridging sites, respectively, and have been corroborated by literature. It was also determined through this study that monitoring the RAIRS peak intensity would not be enough to determine concentration because of how CO binds to the metal surface. When looking at the slightly more complicated surface of (2 × 1)-O/Rh (111) and CO, the results showed only a peak corresponding to the atop position around 2070 cm^{-1}. Even through the initial studies it is clear that the integration of RAIRS into the experimental setup has

shed light on the nuances of surface molecular interactions that we were not previously able to see with TPD/LEED/STM alone.

Future directions for this project include expanding the types of oxygenated surfaces to larger θ_O with atomic oxygen at high temperature (700 K) and low temperature (350 K) exposures. We hypothesize that as the oxygen coverage increases, the amount of CO binding sites on the surface will decrease due to the lack of atop and bridge sites available. Preliminary experiments do show indication of this occurring, but a deeper look into the IR frequencies location and intensities have yet to investigated. It would also be beneficial to look at these oxygenated surfaces with other surface science techniques. MAES will allow for a closer quantitative analysis of oxygen on the surface. LEED would allow for a rapid analysis of surface adsorbate structures. And STM would allow real space, subatomic resolution image of the many different surface environments.

REFERENCE LIST

1. Norskov, J. K.; Studt, Felix.; Abild-Pedersen, F.; Bligaard, Thomas., *Fundamental Concepts in Heterogeneous Catalysis;* John Wiley & Sons, Inc., Hoboken, NJ, **2014**.

2. Kolasinski, K. W. *Surface Science: Foundations of Catalysis and Nanoscience*, Second Edi.; John Wiley & Sons Inc., West Chester, PA, **2008**.

3. Ertl, G. Primary Steps in Catalytic Synthesis of Ammonia. *JVST* **1982**, *1*, 1247–1253.

4. Smil, V. Detonator of the Population Explosion. *Nature* **1999**, *400*, 415.

5. Derouin, J.; Farber, R. G.; Killelea, D. R. Combined STM and TPD Study of Rh(111) under Conditions of High Oxygen Coverage. *J. Phys. Chem* **2015**, *119*, 14748–14755.

6. Freund, H.-J.; Kuhlenbeck, H.; Libuda, J.; Rupprechter, G.; Bäumer, M.; Hamann, H. Bridging the Pressure and Materials Gaps between Catalysis and Surface Science: Clean and Modified Oxide Surfaces, *Top Catal* **2001**, 15.

7. Blomberg, S.; Hejral, U.; Shipilin, M.; et al. Bridging the Pressure Gap in CO Oxidation. *ACS Catal* **2021**, *11*, 9128–9135.

8. Rupprechter, G.; Weilach, C. Mind the Gap! Spectroscopy of Catalytically Active Phases. *NanoToday* **2007**, *2*, 20–29.

9. Gustafson, J.; Westerström, R.; Balmes, O.; et al. Catalytic Activity of the RH Surface Oxide: CO Oxidation over Rh (111) under Realistic Conditions. *J Phys Chem* **2010**, *114* (10), 4580–4583.

10. Topsoe, H. Developments in Operando Studies and in Situ Characterization of Heterogeneous Catalysts. *J Catal* **2003**, *216*, 155–164.

11. Gao, F.; Goodman, D. W. Model Catalysts: Simulating the Complexities of Heterogeneous Catalysts. *Annu Rev Phys Chem* **2012**, *63*, 265–286.

12. Somorjai, G. A.; Li, Y. *Introduction to Surface Chemistry and Catalysis*, Second Edi.; John Wiley & Sons, Inc., Hoboken, NJ, **2010.**

13. Thiel, P. A.; Yates Jr, J. T.; Weinberg, W. H. The Interaction of Oxygen with the Rh(111) Surface. *Surf Sci* **1979**, *82* (1), 22–44.

14. Montemore, M. M.; van Spronsen, M. A.; Madix, R. J.; Friend, C. M. O2 Activation by Metal Surfaces: Implications for Bonding and Reactivity on Heterogeneous Catalysts. *Chem Rev* **2018**, *118*, 2816–2862.

15. Köhler, L.; Kresse, G.; Schmid, M.; et al. High-Coverage Oxygen Structures on Rh(111): Adsorbate Repulsion and Site Preference Is Not Enough. *Phys Rev Lett* **2004**, *93*.

16. Langmuir, I. Adsorption of Gases on Glass, Mica and Platinum. *J Am Chem Soc* **1918**, *40*, 1361–1404.

17. Jones, T. E.; Rocha, T. C. R.; Knop-Gericke, A.; Stampfl, C.; Schlögl, R.; Piccinin, S. Thermodynamic and Spectroscopic Properties of Oxygen on Silver under an Oxygen Atmosphere. *Phys Chem Chem Phys* **2015**, *17* (14), 9288–9312.

18. Bao, X.; Barth, J. V.; Lehmphfuhl, G.; Schuster, R.; Uchida, Y.; Schlogl, R.; Ertl, G. Oxygen-Induced Restructuring of Ag(111). *Surf Sci* **1993**, *284* (1–2), 14–22.

19. Lundgren, E.; Gustafson, J.; Resta, A.; Weissenrieder, J.; Mikkelsen, A.; Andersen, J. N.; Köhler, L.; Kresse, G.; Klikovits, J.; Biederman, A.; Schmid, M.; Varga, P. The Surface Oxide as a Source of Oxygen on Rh(111). *J. Electron Spectrosc. Relat. Phenom;* **2005**; Vol. 144–147, 367–372.

20. Weaver, J. F. Surface Chemistry of Late Transition Metal Oxides. *Chem Rev* **2013**, *113* (6), 4164–4215.

21. Lundgren, E.; Mikkelsen, A.; Andersen, J. N.; Kresse, G.; Schmid, M.; Varga, P. Surface Oxides on Close-Packed Surfaces of Late Transition Metals. *J Phys Condens Matter*. August 2, 2006.

22. Badan, C.; Farber, R. G.; Heyrich, Y.; Koper, M. T. M.; Killelea, D. R.; Juurlink, L. B. F. Step-Type Selective Oxidation of Platinum Surfaces. *J Phys Chem C* **2016**, *120* (40), 22927–22935.

23. Schalow, T.; Laurin, M.; Brandt, B.; Schauermann, S.; Guimond, S.; Kuhlenbeck, H.; Starr, D. E.; Shaikhutdinov, S. K.; Libuda, J.; Freund, H. J. Oxygen Storage at the Metal/Oxide Interface of Catalyst Nanoparticles. *Angew Chem Int Ed* **2005**, *44* (46), 7601–7605.

24. Zhang, F.; Li, T.; Pan, L.; Asthagiri, A.; Weaver, J. F. CO Oxidation on Single and Multilayer Pd Oxides on Pd(111): Mechanistic Insights from RAIRS. *Catal Sci Technol* **2014**, *4* (11), 3826–3834.

25. Devarajan, S. P.; Hinojosa, J. A.; Weaver, J. F. STM Study of High-Coverage Structures of Atomic Oxygen on Pt(1 1 1): P(2 × 1) and Pt Oxide Chain Structures. *Surf Sci* **2008**, *602* (19), 3116–3124.

26. Lundgren, E.; Kresse, G.; Klein, C.; Borg, M.; Andersen, J. N.; de Santis, M.; Gauthier, Y.; Konvicka, C.; Schmid, M.; Varga, P. Two-Dimensional Oxide on Pd(111). *Phys Rev Lett* **2002**, *88* (24), 2461031–2461034.

27. Lundgren, E.; Gustafson, J.; Resta, A.; Weissenrieder, J.; Mikkelsen, A.; Andersen, J. N.; Köhler, L.; Kresse, G.; Klikovits, J.; Biederman, A.; Schmid, M.; Varga, P. The Surface Oxide as a Source of Oxygen on Rh(111). *J. Electron Spectrosc. Relat. Phenom;* **2005**; Vol. 144–147, 367–372.

28. Bardi, U.; Caporali, S. Precious Metals in Automotive Technology: An Unsolvable Depletion Problem? *Minerals* **2014**, *4* (2), 388–398.

29. Farber, R. G.; Turano, M. E.; Killelea, D. R. Identification of Surface Sites for Low-Temperature Heterogeneously Catalyzed CO Oxidation on Rh(111). *ACS Catal* **2018**, *8* (12), 11483–11490.

30. Horn, R.; Williams, K. A.; Degenstein, N. J.; Schmidt, L. D. Syngas by Catalytic Partial Oxidation of Methane on Rhodium: Mechanistic Conclusions from Spatially Resolved Measurements and Numerical Simulations. *J Catal* **2006**, *242* (1), 92–102.

31. Schwegmann, S.; Over, H.; de Renzi, V.; Ertl, G. The Atomic Geometry of the O and CO + O Phases on Rh(Lll); *Surf Sci* **1997**, *375*, 91-106.

32. Marchini, S.; Sachs, C.; Wintterlin, J. STM Investigation of the (2 × 2)O and (2 × 1)O Structures on Rh(1 1 1). *Surf Sci* **2005**, *592* (1–3), 58–64.

33. Farber, R. G.; Turano, M. E.; Oskorep, E. C. N.; Wands, N. T.; Iski, E. v.; Killelea, D. R. The Quest for Stability: Structural Dependence of Rh(111) on Oxygen Coverage at Elevated Temperature. *J Phys Chem C* **2017**, *121* (19), 10470–10475.

34. Grant, J.; Haas, T. A Study of Ru(0001) and Rh(111) Surfaces Using LEED and Auger Electron Spectroscopy. *Surf Sci* **1970**, *21*, 76–85.

35. Kittel, C. *Introduction to Solid State Physics*, Eighth Edi.; John Wiley & Sons, Inc., Hoboken, NJ, **2005**.

36. Gibson, K. D.; Killelea, D. R.; Sibener, S. J. Comparison of the Surface and Subsurface Oxygen Reactivity and Dynamics with Co Adsorbed on Rh(111). *J Phys Chem C* **2014**, *118* (27), 14977–14982.

37. Turano, M. E.; Jamka, E. A.; Gillum, M. Z.; Gibson, K. D.; Farber, R. G.; Walkosz, W.; Sibener, S. J.; Rosenberg, R. A.; Killelea, D. R. Emergence of Subsurface Oxygen on Rh(111). *J Phys Chem Lett* **2021**, *12*.

38. Mavrikakis, M.; Rempel, J.; Greeley, J.; Hansen, L. B.; Nørskov, J. K. Atomic and Molecular Adsorption on Rh(111). *Chem Phys* **2002**, *117* (14), 6737–6744.

39. Castnerm D; Sexton, B.; Somorjai, G. LEED and Thermal Desportion Studies of Small Molecules (H2, O2, CO, CO2, NO, C2H4, C2H2, and C) CHemisorbed on Rhodium (111) and (100). *Surf Sci* **1978**, *71*, 519–540.

40. Freund, H. J. The Surface Science of Catalysis and More, Using Ultrathin Oxide Films as Templates: A Perspective. *J Am Chem Soc* **2016**, *138* (29), 8985–8996.

41. Ganduglia-Pirovano, M. v; Scheffler, M. Structural and Electronic Properties of Chemisorbed Oxygen on Rh(111). *Phys Rev B* **1999**, *59* (23), 15533–15543.

42. Gibson, K. D.; Viste, M.; Sanchez, E.; Sibener, S. J. Physical and Chemical Properties of High Density Atomic Oxygen Overlayers under Ultrahigh Vacuum Conditions: (1 x 1)-O/Rh(111). *Journal of Chemical Physics* **2000**, *112* (5), 2470–2478.

43. Derouin, J.; Farber, R. G.; Heslop, S. L.; Killelea, D. R. Formation of surface oxides and Ag2O thin films with atomic oxygen on Ag(111). *Surf Sci* 2015. *641*, L1-L4.

44. Flege, J. I.; Sutter, P. In Situ Structural Imaging of CO Oxidation Catalysis on Oxidized Rh(111). *Phys Rev B Condensed Matter* **2008**, *78* (15).

45. Blomberg, S.; Lundgren, E.; Westerström, R.; Erdogan, E.; Martin, N. M.; Mikkelsen, A.; Andersen, J. N.; Mittendorfer, F.; Gustafson, J. Structure of the Rh2O3(0001) Surface. *Surf Sci* **2012**, *606* (17–18), 1416–1421.

46. Gustafson, J.; Westerström, R.; Balmes, O.; Resta, A.; van Rijn, R.; Torrelles, X.; Herbschleb, C. T.; Frenken, J. W. M.; Lundgren, E. Catalytic Activity of the RH Surface Oxide: CO Oxidation over RH(111) under Realistic Conditions. *J Phys Chem C* **2010**, *114* (10), 4580–4583.

47. Gustafson, J.; Westerström, R.; Resta, A.; Mikkelsen, A.; Andersen, J. N.; Balmes, O.; Torrelles, X.; Schmid, M.; Varga, P.; Hammer, B.; Kresse, G.; Baddeley, C. J.; Lundgren, E. Structure and Catalytic Reactivity of Rh Oxides. *Catal Today* **2009**, *145* (3–4), 227–235.

48. Montemore, M. M.; van Spronsen, M. A.; Madix, R. J.; Friend, C. M. O2 Activation by Metal Surfaces: Implications for Bonding and Reactivity on Heterogeneous Catalysts. *Chem Rev* **2018**, *118* (5), 2816–2862.

49. Krenn, G.; Bako, I.; Schennach, R. CO Adsorption and CO and O Coadsorption on Rh(111) Studied by Reflection Absorption Infrared Spectroscopy and Density Functional Theory. *Chem Phys* **2006**, *124* (14).

50. Kizilkaya, A. C.; Gracia, J. M.; Niemantsverdriet, J. W. A Direct Relation between Adsorbate Interactions, Configurations, and Reactivity: CO Oxidation on Rh(100) and Rh(111). *J Phys Chem C* **2010**, *114* (49), 21672–21680.

51. Linke, R.; Curulla, D.; Hopstaken, M. J. P.; Niemantsverdriet, J. W. CO/Rh(111): Vibrational Frequency Shifts and Lateral Interactions in Adsorbate Layers. *Chem Phys* **2001**, *115* (17), 8209–8216.

52. Hopstaken, M. J. P.; Niemantsverdriet, J. W. Structure Sensitivity in the CO Oxidation on Rhodium: Effect of Adsorbate Coverages on Oxidation Kinetics on Rh(100) and Rh(111). *Chem Phys* **2000**, *113* (13), 5457–5465.

53. Turano, M. E.; Farber, R. G.; Hildebrandt, G.; Killelea, D. R. Temperature Dependence of CO Oxidation on Rh(111) by Adsorbed Oxygen. *Surf Sci* **2020**, *695*.

54. Trenary, M. Reflection Absorption Infrared Spectroscopy and the Structure of Molecular Adsorbates on Metal Surfaces. *Annu Rev Phys Chem* **2000**, *51* (1), 381–403.

55. Chabal, Y. J. Surface Infrared Spectroscopy. *Surf Sci Reports* **1988**, *8*, 311–357.

56. Fan, J.; Trenary, M. Symmetry and the Surface Infrared Selection Rule for the Determination of the Structure of Molecules on Metal Surfaces. *Langmuir* **1994**, *10* (10), 3649–3657.

57. Choi, J.; Pan, L.; Zhang, F.; Diulus, J. T.; Asthagiri, A.; Weaver, J. F. Molecular Adsorption of NO on PdO(101). *Surf Sci* **2015**, *640*, 150–158.

58. Weaver, J. F.; Choi, J.; Mehar, V.; Wu, C. Kinetic Coupling among Metal and Oxide Phases during CO Oxidation on Partially Reduced PdO(101): Influence of Gas-Phase Composition. *ACS Catal* **2017**, *7* (10), 7319–7331.

59. Waluyo, I.; Ren, Y.; Trenary, M. Observation of Tunneling in the Hydrogenation of Atomic Nitrogen on the Ru(001) Surface to Form NH. *J Phys Chem Lett* **2013**, *4* (21), 3779–3786.

60. Hollins, P.; Pritchard, J. Infrared Studies of Chemisorbed Layers on Single Crystals. *Prog Surf Sci* **1966**, *19* (4), 276–350.

61. Mudiyanselage, K.; Stacchiola, D. *In-Situ Characterization of Heterogeneous Catalysts*, 1st Edition.; Chupas, P., Hanson, J., Rodriguez, J., Eds.; John Wiley & Sons: Hoboken, New Jersey, **2013.**

62. Liang, Z.; Yang, H. J.; Oh, J.; Jung, J.; Kim, Y.; Trenary, M. Atomic-Scale Dynamics of Surface-Catalyzed Hydrogenation/Dehydrogenation: NH on Pt(111). *ACS Nano* **2015**, *9* (8), 8303–8311.

63. Zhou, J. H.; Sui, Z. J.; Zhu, J.; Li, P.; Chen, D.; Dai, Y. C.; Yuan, W. K. Characterization of Surface Oxygen Complexes on Carbon Nanofibers by TPD, XPS and FT-IR. *Carbon N Y* **2007**, *45* (4), 785–796.

64. Soy, E.; Liang, Z.; Trenary, M. Formation of Pt and Rh Nanoclusters on a Graphene Moire´ Pattern on Cu(111). *J Phys Chem C* **2015**, *119* (44), 24796–24803.

65. Jentz, D.; Trenary, M.; Peng, X. D.; Stair, P. The Thermal Decomposition of Azomethane on Pt(111) *Surf Sci* **1995**, *341*.

66. Xu, J.; Yates, J. T. Terrace Width Effect on Adsorbate Vibrations: A Comparison of Pt(335) and Pt(Ll2) for Chemisorption of CO *Surf Sci* **1995**, *327*.

67. Kruppe, C. M.; Krooswyk, J. D.; Trenary, M. Polarization-Dependent Infrared Spectroscopy of Adsorbed Carbon Monoxide To Probe the Surface of a Pd/Cu(111) Single-Atom Alloy. *J Phys Chem C* **2017**, *121* (17), 9361–9369.

68. Patel, D. A.; Hannagan, R. T.; Kress, P. L.; Schilling, A. C.; Çlnar, V.; Sykes, E. C. H. Atomic-Scale Surface Structure and CO Tolerance of NiCu Single-Atom Alloys. *J Phys Chem C* **2019**, *123* (46), 28142–28147.

69. MMRC. *5.12 Vibrational Surface Spectroscopy*. https://mmrc.caltech.edu/LK EELS/LK HREELS.html.

70. Martin, N. M.; Van Den Bossche, M.; Grönbeck, H.; Hakanoglu, C.; Zhang, F.; Li, T.; Gustafson, J.; Weaver, J. F.; Lundgren, E. CO Adsorption on Clean and Oxidized Pd(111). *J Phys Chem C* **2014**, *118* (2), 1118–1128.

71. Gerrard, A. L.; Weaver, J. F. Kinetics of CO Oxidation on High-Concentration Phases of Atomic Oxygen on Pt(111). *J Chem Phys* **2005**, *123* (22).

72. Curulla, D.; Linke, R.; Clotet, A.; Ricart, J. M.; Niemantsverdriet, J. W. Assignment of the Vibrational Features in the Rh(1 1 1)-(2 Â 2)-3CO Adsorption Structure Using Density Functional Theory Calculations. *Chem Phys Lett* **2002**, *354*, 503–507.

73. Nakamura, I.; Kobayashi, Y.; Hamada, H.; Fujitani, T. Adsorption Behavior and Reaction Properties of NO and CO on Rh(1 1 1). *Surf Sci* **2006**, *600* (16), 3235–3242.

74. Köhler, L.; Kresse, G. Density Functional Study of CO on Rh(111) [78]. *Phy Rev B* **2004**, *70* (16), 1–9.

75. King, D. A. Thermal Desorption From Metal Surfaces: A Review. *Surf Sci* **1975**, *47*, 384–402.

76. Redhead, P. A. Thermal Desorption of Gases. *Vacuum* **1962**, 203–211.

77. Weinert, F. Davisson—Germer Experiment. *Compendium of Quantum Physics*; Greenberger, D., Hentschel, K., Weinert, F., Eds.; Springer: Berlin, Heidelberg, 2009; 150–152.

78. Kan, H. H.; Shumbera, R. B.; Weaver, J. F. Adsorption and Abstraction of Oxygen Atoms on Pd(1 1 1): Characterization of the Precursor to PdO Formation. *Surf Sci* **2008**, *602* (7), 1337–1346.

79. Kan, H. H.; Weaver, J. F. A PdO(1 0 1) Thin Film Grown on Pd(1 1 1) in Ultrahigh Vacuum. *Surf Sci* **2008**, *602* (9), 1–5.

80. Freund, H. J.; Somorjai, G. A. The Frontiers of Catalysis Science and Future Challenges. *Catal Lett* **2015**, 1–2.

81. Ye, R.; Hurlburt, T. J.; Sabyrov, K.; Alayoglu, S.; Somorjai, G. A. Molecular Catalysis Science: Perspective on Unifying the Fields of Catalysis. *Proc Natl Acad Sci* **2016**, 5159–5166.

82. Park, B. G.; Kitsopoulos, T.; Borodin, D.; Golibrzuch, K.; Auerbach, D. J.; Campbell, C. T.; Wodtke, A. M. The Kinetics of Elementary Thermal Reactions in Heterogeneous Catalysis. *Nat Rev Chem* **2019**, *3* (12), 723-732.

83. Neugebohren, J.; Borodin, D.; Hahn, H. W.; et al. Velocity-Resolved Kinetics of Site-Specific Carbon Monoxide Oxidation on Platinum Surfaces. *Nature* **2018**, *558* (7709), 280–283.

84. Brown, L. S.; Sibener, S. J. A Molecular Beam Scattering Investigation of the Oxidation of CO on Rh(111) Angular and Velocity Distributions of the CO2 Product. *J Chem Phys* **1989**, *90* (5), 2807–2815.

85. Hopster, H.; Ibach, H.; Comsa, G. Catalytic Oxidation of Carbon Monoxide on Stepped Platinum(111) Surfaces. *J Catal.* **1977**, *46* (1), 37–48.

86. Jaworowski, A. J.; Beutler, A.; Strisland, F.; Nyholm, R.; Setlik, B.; Heskett, D.; Andersen, J. N. Adsorption Sites in O and CO Coadsorption Phases on Rh(111) Investigated by High-Resolution Core-Level Photoemission *Surf Sci* **1999**; 431, 33-41.

87. Jansen, M. M. M.; Scheijen, F. J. E.; Ashley, J.; Nieuwenhuys, B. E.; Niemantsverdriet, J. W. Adsorption/Desorption Studies of CO on a Rhodium(1 0 0) Surface under UHV Conditions: A Comparative Study Using XPS, RAIRS, and SSIMS. *Catal Today* **2010**, *154* (1–2), 53–60.

88. Krooswyk, J. D.; Yin, J.; Asunskis, A. L.; Hu, X.; Trenary, M. Spectroscopic Evidence for a CO – O2 Complex as a Precursor to the Low Temperature Oxidation of CO on the Pt (111) Surface. *Chem Phys Lett* **2014**, *593*, 204–208.

89. Zhou, L.; Kandratsenka, A.; Campbell, C. T.; Wodtke, A. M.; Guo, H. Origin of Thermal and Hyperthermal CO 2 from CO Oxidation on Pt Surfaces: The Role of Post-Transition-State Dynamics, Active Sites, and Chemisorbed CO2. *Angew Chem* **2019**, *131* (21), 6990–6994.

90. Park, G.; et al. Fundamental Mechanisms for Molecular Energy Conversion and Chemical Reactions at Surfaces. *Rep Prog Phys* **2019**, *82*.

91. Liang, Z.; Li, T.; Kim, M.; Asthagiri, A.; Weaver, J. F. Low-Temperature Activation of Methane on the IrO2 (110) *Surf Sci* **2017**, *356* (6335), 299–303.

92. Gibson, K., Colonell, J., and Sibener, S. J. *Surf Sci* **1995**, 343 (1-2), L1151-L1155.

93. Thiel, P.; Williams, E.; Yates, J.; Weinberg, W. The Chemisorption of Co on Rh(111). *Surf Sci* **1979**, *84* (1), 54–64.

94. Föhlisch, A.; Nyberg, M.; Bennich, P.; Triguero, L.; Hasselström, J.; Karis, O.; Pettersson, L. G. M.; Nilsson, A. The Bonding of CO to Metal Surfaces. *J Chem Phys* **2000**, *112* (4), 1946–1958.

95. Gunathunge, C. M.; Li, J.; Li, X.; Waegele, M. M. Surface-Adsorbed CO as an Infrared Probe of Electrocatalytic Interfaces. *ACS Catal.* **2020**, *10* (20), 11700–11711.

VITA

Dr. Elizabeth Jamka was born and raised in Addison, Illinois. Before attending Loyola University Chicago, she attended Elmhurst University (formally Elmhurst College), in Elmhurst, Illinois where she earned a Bachelor of Science in Chemistry, with Honors, in 2015.

While at Loyola, Dr. Jamka was a teaching assistant for many different teaching laboratories. She also won the department Teaching Assistant of the year in 2020. Dr. Jamka was a Teaching Scholars Fellow for the 2021-2022 academic year, where she mentors other graduate students who were instructors of record for the first time. Dr. Jamka volunteered working with high school students in their science classes and was an active Chicago area alumni volunteer and chapter advisor for Alpha Phi Omega, a volunteer-based service organization.